Published in final edited form as:
J Immunol. 2013 June 1; 190(11): 5874–5881. doi:10.4049/jimmunol.1202612.

Radiation-induced equilibrium is a balance between tumor cell proliferation and T cell-mediated killing

Hua Liang[1,*], **Liufu Deng**[1,*], **Steven Chmura**[1], **Byron Burnette**[2], **Nicole Liadis**[1], **Thomas Darga**[1], **Michael A. Beckett**[1], **Mark W. Lingen**[2], **MaryEllyn Witt**[1], **Ralph R. Weichselbaum**[1], and **Yang-Xin Fu**[2]

[1]Department of Radiation and Cellular Oncology, The Ludwig Center for Metastasis Research

[2]Department of Pathology, University of Chicago, Chicago, IL 60637

Abstract

Local failures following radiation therapy are multifactorial and the contributions of the tumor and the host are complex. Current models of tumor equilibrium suggest that a balance exists between cell birth and cell death due to insufficient angiogenesis, immune effects, or intrinsic cellular factors. We investigated whether host immune responses contribute to radiation induced tumor equilibrium in animal models. We report an essential role for immune cells and their cytokines in suppressing tumor cell regrowth in two experimental animal model systems. Depletion of T cells or neutralization of interferon-gamma reversed radiation-induced equilibrium leading to tumor regrowth. We also demonstrate that PD-L1 blockade augments T cell responses leading to rejection of tumors in radiation induced equilibrium. We identify an active interplay between tumor cells and immune cells that occurs in radiation-induced tumor equilibrium and suggest a potential role for disruption of the PD-L1/PD-1 axis in increasing local tumor control.

Keywords

radiation; stable disease; immunity; equilibrium

INTRODUCTION

Clinical stable disease has several manifestations that are broadly characterized by the failure of tumors to progress and instead remain static over variable periods of time (1–2). Mechanistically, stable disease could result from induction of cellular dormancy, the failure of tumor cells to proliferate and instead adopt a temporary state of quiescence, or an equilibrium process of balanced cell proliferation and cell death. Tumors that receive radiation therapy (RT) sometimes exhibit a progression-free period of stable disease with subsequent late relapse. However, the mechanisms that contribute to both the induction and maintenance of a stable disease state as well as late failures following radiotherapy are poorly understood. Evidence from various clinical trials across multiple tumor types indicates that local failures often occur after several years. For example, analysis of

Corresponding authors: Ralph Weichselbaum (rrw@radonc.uchicago.edu). And Yang-xin Fu (yfu@uchicago.edu).
*These authors contributed equally to this work.

Competing interests: The authors declare that no conflict of interest exists.

Authors contribution: H.L. and L.F.D. performed the experiments and wrote the paper. S.C., M.W.L. and M.W. aided in clinic experiments. B.B., M.B. and N.L. aided in certain animal experiments. H.L., L.F.D., S.C., B.B., M.W.L. M.W., M.B. and N.L. analyzed the data. B.B. helped in the editing the manuscript. R.R.W and Y.X.F conceived of and supervised all experiments and the writing of the manuscript. All authors approved the paper.

randomized trials comprising 11,000 women with early stage breast cancer treated with surgery and radiotherapy demonstrated that over 50% of the local failures occurred after 5 years with 25% occurring after 10 years (3). Similarly, the long-term results of a phase III RTOG (85–31) trial in prostate cancer comparing radiotherapy with or without androgen deprivation demonstrated that over 50% of the local failures occur 5 years after treatment (4). Other disease types also demonstrate late failures following radiotherapy including 15% for uveal melanoma patients at 6 years (5) and 13% for head and neck cancer at 2 years post radiotherapy (6). One prevailing view is that the duration of progression-free/stable disease is determined by the number of surviving clonogens and tumor repopulation (e.g fewer surviving clonogens) take longer to repopulate). Therefore the extent of initial tumor cell or stromal killing by radiation is proposed to, in part, mediate the time to relapse. However an alternative explanation is the induction of tumor equilibrium. Equilibrium is a state whereby tumor proliferation is balanced by cell death, and both angiogenic, and immunological mechanisms have been demonstrated to mediate tumor equilibrium (7–8). The induction of equilibrium could therefore represent a temporarily stable, yet transitional, disease state wherein tumor progression is halted, but from which tumors eventually escape to relapse locally at variable intervals.

Immunologically based equilibrium was reported in a carcinogen-induced animal tumor model wherein the maintenance of small stable tumors was associated with the establishment of an equilibrium state (9). Here, we report that radiation therapy induces prolonged stable or partial clinical responses that are characterized by coincidence of actively proliferating tumor cells and pronounced immune infiltration resulting in Radiation-Induced Tumor Equilibrium (RITE). Using animal model systems, we identify one possible mechanism for RITE as an active balance of two dynamic processes: tumor cell proliferation and apoptosis that is mediated by local immune cells. These results suggest that immunotherapy may strengthen limited immunity and tip the balance toward improved eradication of residual cancer cells.

MATERIALS AND METHODS

Human subjects and Clinical Trials

The oligometastasis trial was approved by the University of Chicago Institutional Review Board (Approval #13619B), and the Institutional Review Board-approved written informed consent was obtained from each patient before protocol therapy. Patients eligible for this trial were described previously(10–11). Declaration of Helsinki protocols were followed.

Mice and Cell Lines

C57BL6 and Balb/c mice were purchases from Harlan at 6 to 7 weeks of age. All the mice were maintained under specific pathogen free conditions and used in accordance to the animal experimental guidelines set by the Institute of Animal Care and Use Committee. This study has been approved by the Institutional Animal Care and Use Committee of the University of Chicago. B16-SIY melanoma cells were obtained from Tom Gajewski (University of Chicago) and maintained by R.R.W. and Y-.X.F(12). TUBO was cloned from a spontaneous mammary tumor in a BALB neu Tg mice (13). 3T3KB and 3T3NKB were gifted from Dr. Wei-Zen Wei, Wayne State University (13). 3T3KB mouse fibroblasts express H-2K^{d} and B7.1, and 3T3NKB cells express additional Her-2 or neu.

Tumor Growth and Treatments

Single tumor cell suspension was harvested from cultured cells. 5×10^{5} cells were injected as described (13). Tumor volumes were measured along three orthogonal axes (a, b, and c) and calculated as tumor volume = abc/2. Tumors were allowed to grow for about 2 weeks when

the size reached 50–150 mm^3 before treated with local RT(12). In general, the more radiosensitive TUBO tumors received 15 Gy, and the more radioresistant B16SIY tumors received 2 doses of 25 Gy. Tumor volumes were measured every 3–4 days. To select stable equilibrium tumors, we investigated tumors between 50–150mm^3 in all the depletion experiments. For antibody mediated cell depletions, 200μg per mouse of anti-CD4 (clone GK1.5) and/or anti-CD8 (clone 24.3.1, Fitch Monoclonal Antibody Facility, The University of Chicago) were delivered 3 times by i.p. injection at 5 day intervals. For PD-L1 blockade experiments, 200μg anti-PD-L1(clone 10F.9G2, BioXCell) was administered i.p. every three days for a total of four times to mice bearing stable tumors (defined at three weeks after RT). For IFNγ blockade experiments, mice bearing stable tumors were injected i.p. with 500μg anti-IFNγ (clone XMG1.2, BioXCell) or isotype control every 5 days for a total of three injections.

Immunohistochemistry

Frozen mouse tumor tissue was treated with acetone/methanol for 20 minutes prior to CD8 (clone 53–6.7, BioLegend) staining. Sections were treated with picric acid formalin fixative for 10 minutes for Ki-67 staining (1:75, clone TEC-3, DAKO). After incubation with biotinylated anti-rat IgG (Vector laboratories), sections were labeled using the Elite kit (Vector Laboratories) and DAB (DAKO) system. Tissue sections were counterstained and mounted. The slides were scanned at 20× magnification using Aperio ScanScope XT, and viewed using Aperio ImageScope. TUBO tumor slides were annotated and analyzed using Aperio ImageScope. Ten random high power fields were selected for $CD8^+$ and $Ki67^+$ staining respectively. TUNEL signal was analyzed in the same selected area. All the staining was performed on sequential slides from 3 individual mouse tumors.

Ex-vivo Radiosensitivity assay

Fourteen days after tumor cell implantation, TUBO tumors, which measured 50–200mm^3 in size, were subjected to 15 Gy radiation. Tumors were measured every three days and their responses to RT were characterized as non-responsive (NR) or responsive (R) after day 6 post RT. Eight days post RT, 3 tumors from the non-RT control, NR, and R were removed and digested with collagenase into single cell suspensions. Plated cells from each tumor were allowed to grow for 2 days and were then subjected to 0 Gy, 5 Gy or 10 Gy radiation. Colonies were stained with crystal violet and those larger than 50 cells were counted 10 days after plating. The relative surviving fractions after 5 or 10 Gy were calculated as fold change over colony numbers from the 0 Gy control of the same tumor sample. In the same study, stable (S) and late escapers/partial responding (PR) tumors were excised and subjected to the same radiosensitivity assay as described above.

Cell Sorting and qRT-PCR

Tumors were disassociated, stained and sorted as described (14). Flow Sorted Cells were homogenized in 800ul Trizol LS. RNA isolation was performed following the manufacturer's instructions with the addition of glycogen. cDNA was synthesized using 10uL of RNA by using the High Capacity cDNA Reverse Transcription Kit (Applied Biosystems). A mock RT control reaction was also performed using 10uL of RNA. qPCR was performed on an ABI 7900HT (Applied Biosystems) using Power SYBR Green PCR Master Mix (Applied Biosystems). Gene fold change calculations were performed using the comparative Ct method, GAPDH was used as the endogenous gene control. Primer sequences:

IFNG-f -tgagctcattgaatgcttgg; IFNG-r -acagcaaggcgaaaaaggat;

STAT1-f -agtcggaggccctaatgct; STAT1-r ccataatgcacccatcattcca;

GAPDH-f –aacgacccttcattgac; GAPDH-r -tccacgacatactcagcac

IFIT3-f –agtgaggtcaaccgggaatct; IFIT3-r -tctaggtgctttatgtaggcca

CD274(PDL1)-f–gcctgctgtcacttgctacggg; CD274(PDL1)-r –cagcgaggctctccccctga.

ELISPOT and CBA Assay

Tumor draining lymph nodes and tumors were removed, and prepared into single cell suspensions as described (12). Tumor infiltrating lymphocytes (TILs) were purified using Ficoll gradient centrifugation (GE). 96-well HTS-IP plates (Millipore) were pre-coated with 5μg/ml anti-IFNγ antibody (clone R4-6A2, BD Pharmingen) overnight at 4°C. 1–3×10^5 lymph node cells or TILs (harvested at day 40 after RT) were cocultured with 3T3NKB cells at a ratio of 10:1 in the presence (for TILs) or absence of 25 IU/ml IL-2. 3T3KB cells were used as a control cell line for antigen specificity. After 3 days of incubation, cells were removed, 4μg/ml biotinylated anti-IFNγ antibody (clone XMG1.2, BD Pharmingen) was added, and the plate was incubated for 2h at 37°C. 0.9μg/ml avidin-horseradish peroxidase (BD Pharmingen) was then added and the plate was incubated for 45 min at 37 °C. The cytokine spots were developed according to product protocol (Millipore). Supernatants from the flat-bottom 96-well plate, where TILs were stimulated with 3T3NKB or 3T3KB cells as described above, were subjected to BD CBA assay to detect cytokines according to the instruction manual.

Flow Cytometry

To obtain single cell suspensions, tumor tissues were digested with 1mg/ml Collagenase IV (Sigma) and 0.2 mg/ml DNase I (Sigma) for 45 min at 37 °C. Cells were stained with antibodies specific for CD8, CD4 and CD45 (BioLegend). Samples were analyzed on a FACSCalibur Flow Cytometer (BD) and data were analyzed with FlowJo Software (TreeStar).

Statistical Analysis

Data were analyzed using Prism 5.0 Software (GraphPad). Experiments were repeated two or three times. The p values were assessed using two-tailed unpaired Student *t* tests.

RESULTS

Stable disease is observed in patients with oligometastasis after Stereotactic Body Radiotherapy (ablative radiotherapy) SBRT

Results of a phase I trial demonstrated that patients with metastatic cancer in a limited number of organs (oligometatasis; 1–5 sites) benefited from local high dose per fraction radiotherapy, or SBRT (10–11). Among sixty three (63) patients with less than 3 oligometastasis that received SBRT (36–48Gy)(11), 87% exhibited partial and complete responses resulting in residual tumor nodules that remained progression-free for months or years (4.5–31.4 months mean 20.9 months, Table S1). 31% of these lesions relapsed in the irradiated site. Patients with 1–2 oligometastatic lesions who received SBRT (11), approximately 40% had radiographic freedom from progression for relatively long intervals (Fig. S1A). The relapses observed are consistent with other reports of late failure, suggesting that SBRT induces stable disease in some oligometastatic tumors in a manner similar to primary tumors. Stable disease or prolonged response with relapse was noted in some imaging studies (10–11) As an example, Fig S1B shows a representative patient with metastatic lung cancer that was treated with SBRT and underwent a complete response (CT negative). Five years later the tumor recurred locally, rapidly grew to invade the chest wall, and was confirmed by biopsy (Fig. S1B). The results from our SBRT trial suggested that

ablative RT can induce either a transient or prolonged state of stable disease or cure. It is, therefore, important to study the mechanisms contributing to an arrested state of tumor progression in order to develop new treatment strategies to prevent relapse and mediate complete cure.

Radiotherapy-induced stable disease in murine models

To further our understanding of the mechanisms that contribute to the induction of a stable disease state that precedes late failure, we developed two mouse models. First, TUBO cells derived from a spontaneous breast tumor of BALB-neuT transgenic mice were implanted s.c. in wild type Balb/c mice. TUBO tumors were allowed to establish for 14 days (tumor volume ranged from approximately 50–200mm^3) before receiving 15 Gy, a dose that was determined to result in stable disease in a high fraction of the mice without inducing tissue necrosis. Of the 193 tumors treated across eight independent experiments (Table S2), 45% (87/193) of TUBO tumors remained stable and palpable over a 34 to 60-day period of observation and were classified as stable. The response to RT (15Gy) could be observed as early as 5–7 days post-treatment and tumors could be subdivided into responsive (R) and non-responsive (NR). Of the tumors that demonstrated an early response to RT, 18% (34/193) completely regressed, 14% (27/193) relapsed over the course of 3 weeks (partial response, PR), and 45% (87/193) remained stable (S) for more than 3 weeks. The remaining tumors (23%; 44/193) were not controlled by RT treatment (Non-Responsive, NR).

These different outcomes are summarized in Table S2 and graphically represented in Fig. 1A, B). The spectrum of responses observed in our TUBO mouse model are largely consistent with the range of clinical responses observed after treatment of tumors with radiotherapy. Stable TUBO tumors monitored over the course of 50–80 days post RT can relapse at later time points or remain stable and palpable (Fig. S2 A, B). Induction of stable disease was, in part, dependent on the size of the tumor at the time of local RT delivery and the radiation dose applied. We observed a similar phenotype in larger tumors with average sizes over 200mm^3, however, a higher dose of 20Gy was needed to induce equilibrium(Fig. 1B). We performed similar experiments with B16-SIY melanoma in the C57/BL6 background as described previously (12, 14). B16 is radiation resistant *in vitro* and a higher dose of RT is required to induce stable disease *in vivo*. Two doses of 25Gy were given 10 and 12 days after cell implantation (Fig. 1C). Sixty two percent (18/29) of the tumors remained stable after RT for at least 30 days demonstrating that these observations are not unique to a single tumor model or mouse strain. However, the dose required to achieve a high rate of stable disease is likely related to several factors including the radiosensitivity of the tumor cell lines.

Inherent cellular radiosensitivity is frequently hypothesized to account for the differences observed in the rate of tumor regrowth following treatment of tumors with radiotherapy. To address the potential contribution of differential radiosensitivity to the variability in the responses of TUBO tumors to RT, we determined the radiosensitivity of tumor cells taken from mice that were responsive (R) or non-responsive (NR) to RT. We surgically removed TUBO tumors 8 days post RT and plated tumor cells, which were then assayed for clonogenic survival following delivery of a second dose of RT. The results indicated that at 8 days post RT, tumor cells derived from non-responsive tumors *in vivo* have the same *in vitro* cellular radiosensitivity as the cells from responsive (R) tumors and control tumor cells from un-irradiated mice (Fig. 2A). These results coupled with the fact that the parental TUBO cells have the same *in vitro* radiosensitivity suggest that differences in radiosensitivity do not account for the disparate regrowth kinetics *in vivo* following treatment with local RT. Tumor cells derived from stable tumors (S) and tumors that exhibited a partial response (PR) followed by early relapse at day 21 post RT were subjected to the same assay. Unexpectedly, the tumor cells derived from stable tumors exhibited

equivalent radiosensitivity to cells from tumors that were only partially responsive (Fig. 2B). These results demonstrate that, in our model, the degree of radiosensitivity of tumor cells cannot account for the differential response of tumors to local RT. The results point toward host factors in the maintenance of radiation induced stable disease.

To further characterize our model system, we stained stable TUBO tumor tissues with Ki-67 and TUNEL. There were clusters of Ki-67$^+$ tumor cells adjacent to large areas of TUNEL$^+$ tumor cells suggesting that the tumor cells were both proliferating and dying in the stable tumor nodule and raising the possibility that the stable disease state is achieved through equilibrated rates of division and death (Fig 2C). Furthermore, we noted a prominent T cell infiltration in stable tumors that was dominated by CD8$^+$ T cells. We quantified the number of TUNEL positive cells in randomly selected CD8 and Ki67 positive regions (Fig. 2D). The results show that the TUNEL staining signal is significantly higher in CD8$^+$ areas than in Ki67$^+$ areas ($p=0.001$), suggesting that CD8$^+$ cells could be responsible for the majority of apoptosis in the stable TUBO tumors. Taken together, these data indicate that local ablative RT can induce a stable disease state in two different animal tumor models and that stable disease may result from an equilibrium, that we refer to as radiation induced tumor equilibrium (RITE), between tumor cell proliferation and tumor cell death. Furthermore, the data also raise the possibility that host immune responses might be involved in the generation of the equilibrium and resulting stable disease state.

CD8$^+$ T cells and IFNγ are essential to maintain RT-induced equilibrium

To investigate whether host T cells are required in the induction of stable disease, we depleted CD8$^+$ and CD4$^+$ T cells in mice bearing RITE B16-SIY tumors (Fig. 3A). Tumors in the CD4 and CD8 combined depletion groups showed rapid tumor outgrowth when compared to tumors in non-depleted hosts ($p=0.016$, V/V0. For changes in absolute volume, see Suppl. Fig S2D). We observed similar effects when CD8$^+$ T cells alone were depleted from mice bearing RITE TUBO tumors (Fig. 3B, $P=0.015$, V/V0. For changes in absolute volume, see Suppl. Fig S2E). When examining tumors in which CD8$^+$ cells had been depleted, the fraction of Ki-67$^+$ cells was increased, whereas TUNEL-positive staining was reduced compared to the same staining in non-depleted tumors (data not shown). These data demonstrate that CD8$^+$ T cells play an essential role in maintaining stable disease, in part, through an immunological equilibrium. Consistent with the antibody depletion experiments, TUBO tumors grown in SCID mice, that lack mature B and T cells, couldn't be induced into equilibrium by radiation (Fig. 3C)

TUBO cells grow more aggressively in BALB-nueT Tg mice, from which they were derived, compared to WT Balb/c mice (1334±299 mm^3 vs. 399±183 mm^3 day 33 post tumor implanting, $p=0.04$). The difference in tumor growth kinetics is thought to be due to T cell tolerance against tumor-associated antigens including neu, which is a self or foreign antigen in the BALB-neuT Tg mice and Balb/c mice respectively. To determine whether a heightened state of T cell tolerance in the BALB-neuT Tg mice could affect the induction of radiation-induced equilibrium, we implanted TUBO cells s.c. on the flank of BALB-neuT mice. In 15 days, tumors received 30 Gy locally when the tumor size reached around 100mm^3. Most tumors remained stable for up to 21 days post radiation, before slowly resuming growth (Fig 3D). These results demonstrate that radiation induced equilibrium can be affected by the degree of host T cell tolerance and further implicate T cells as central mediators in RITE.

To begin to understand the role of host immunity in RITE, we investigated multiple mRNA transcripts of immunological significance in sorted populations of infiltrating CD45$^+$ hematopoietic cells and CD45$^-$ tumor cells in stable tumors. CD45$^-$TUBO tumor cells derived from equilibrium tumors expressed high levels of IFN stimulated genes (ISG's) as

determined by quantitative PCR, suggesting an association between increased interferon signaling within the tumor microenvironment and immune-mediated suppression of tumor regrowth (Fig S2C). Mice bearing RITE tumor nodules were treated with anti-IFN-γ neutralizing antibody and showed rapid tumor outgrowth (Fig. 4A, P=0.026. For changes in absolute volume, see Suppl. Fig S2F). Our results are consistent with an earlier report demonstrating the essential role of IFNγ in T cell recruitment and control of primary tumor following local RT (15). These data suggest that RT treatment induces changes in the tumor microenvironment, which facilitate activation of T cells and production of effector cytokines such as IFNγ. To examine antigen-specific T cell responses, tumor antigen specific IFNγ ELISPOT assay was performed on the draining lymph nodes from untreated control mice, mice with non-responsive tumors (NR) or responsive (R) tumors at 1 week following RT, and responsive tumors that remained stable (S) for 5 weeks post-RT. To determine neu-specific responses, 3T3KB and 3T3NKB cells were used as control and neu-specific antigen presenting cells respectively. ELISPOT assay showed an elevated frequency of neu-specific cytokine producing effector T cells in mice harboring responsive (R) tumors when compared to untreated (Non-RT) control tumors or non-responsive tumors (Fig. 4B; p=0.0013). The results demonstrate that the differential response of tumors to RT in individual mice is correlated with the magnitude of the T cell response to tumor antigens.

Although antigen-specific T cell responses were increased significantly in the responsive group (R, 1 week post-RT) compared to that of the non-RT control group (p=0.0013), T cell responses were significantly lower in animals with stable disease (S, 5 weeks post-RT) compared to the animals sacrificed shortly after local radiation (P=0.012, Fig. 4B). The fact that T cell responses declined over a period of 30 days post RT suggests that ongoing T cell priming wanes over time likely as a result of decreased antigen and danger signal release. Compared to the non-irradiated control group, the T cell response from animals with stable disease was still significantly increased in the DLNs (Fig. 4B P=0.02), indicating that the relatively modest T cell response is sufficient to mediate equilibrium but not enough to eliminate the tumor completely. In mice bearing stable tumors, we also observed higher levels of TNFα (Fig. S2G). In addition, the frequency of $CD8^+$ T cells was significantly elevated in responsive tumors compared to non-treated controls but similarly became reduced over time (Fig. 4C). To test whether treated mice that had complete tumor regression maintain a prolonged protection against re-challenge, a critical indication for the control of relapse, mice were re-challenged with the same TUBO tumor cells 30 days after the original tumors were not palpable (approximately 60–70 days post RT). Re-challenged mice failed to grow tumors while naive control mice exhibited aggressive tumor growth (Fig. 4D). Taken together, our data collectively suggest that ablative RT increases the frequency of tumor antigen-specific $CD8^+$ T cells that infiltrate the tumor, but both overall T cell infiltration and cytokine production decrease over time in the tumor microenvironment eventually producing RITE.

Immunotherapy can tip the balance to eradicate stable tumors

We hypothesized that the decline in systemic and local T cell function observed over the course of achieving tumor equilibrium might be a result of gradual T cell exhaustion. T cell exhaustion is a state of T cell dysfunction induced by prolonged exposure to antigenic stimulation and is defined by poor effector function, sustained expression of inhibitory receptors, and a transcriptional state distinct from that of functional effector or memory T cells (16). Therefore, we hypothesized that the equilibrium achieved between proliferating tumor cells and T cell mediated tumor cell death can be tipped to induce complete tumor rejection by either enhancing T cell activation or reducing T cell inhibition to recover the functional capacity of exhausted T cells in the context of tumor equilibrium. Recent studies suggest that PD ligand 1 (PD-L1) expression in human tumor tissues can exhaust T cells

(17–18). We observed an increase in PD-L1 expression in tumor cells from RITE tumors (Fig S2C), concurrent with an increase in systemic effector T cell function in the draining lymph nodes (Fig 4B). We therefore hypothesized that blocking PD-L1 using a neutralizing antibody would release suppression of PD-1^+ T cells within the tumor microenvironment and result in tumor rejection. Indeed, most RITE tumors were rejected after antibody treatment (Fig. 5A, B, p=0.018). Draining lymph nodes were harvested from untreated mice, mice with stable tumors, and mice with stable tumors that were treated with anti-PD-L1 antibody one week after antibody treatment (5 weeks post RT) and subjected to IFNγ ELISPOT assay (Fig. 5C). Antigen specific cytokine release was dramatically increased in mice receiving anti-PD-L1 treatment compared to untreated mice with stable tumors (P=0.002). These data demonstrate that blockade of a T cell negative regulator can increase T cell function to facilitate tumor rejection. These results suggest that tumor equilibrium induced by RT can be disrupted to yield complete regression using immunotherapy.

DISCUSSION

As noted above, previous clinical studies have demonstrated late radiation failures. One hypothesis is that robust cyto-reduction by effective IR induces prolonged regrowth kinetics compared to a less cytoreduced states resulting from lower doses or more radioresistant tumors cells. Here we suggest an alternative explanation for the stable, or disease free, intervals that precede late radiation failures as equilibrium states (radiation-induced tumor equilibrium) generated by a balance between tumor cell proliferation and T cell-mediated killing. Tumors treated with radiotherapy were observed to contain actively proliferating tumor cells and pronounced T cell infiltration. Using animal models of RT-induced tumor equilibrium, we confirmed the essential role of $CD8^+$ T cells in achieving and maintaining progression-free disease since $CD8^+$ T cell depletion led to rapid tumor growth. Conversely, enhancing T cell function through blockade of inhibitory receptors leads to eradication of the remaining tumor. Based on our data, we propose that RITE is dynamically balanced by two opposing mechanisms: aggressive tumor proliferation and $CD8^+$ T cell mediated tumor cell apoptosis.

In TUBO tumor model, intrinsic radiosensitivity of cells from individual tumors did not dictate the response to radiation. To consider the contribution of adaptive immune responses in radioresistence, we conducted experiments in SCID mice. The results are shown in Fig. 3C. TUBO tumors in SCID mice were less responsive than TUBO tumors in immunocompetent Balb/c mice and never reached equilibrium post-radiation. As indicated in the ELISPOT assay, levels of host T cell priming correlated with tumor responses. Our data suggest that local radiation can induce tumor antigen-specific T cell responses in a subset of treated mice, but measureable heterogeneity exists between mice in the induction of tumor-specific immune responses that correlate with local tumor control. At this point we cannot decipher the mechanism(s) underlying the discrepancy of responses in genetically identical hosts (inbred wildtype Balb/c), however, the tumor cells are likely more genetically heterogenous than the mice as a result of intrinsic genomic instability. Alternatively, limited evidence has recently been reported that individual inbred mice, indeed, have different levels of genomic acetylation/methylation that can influence their behavior (19–20). Inbred mice have also been reported to respond differentially to viral infection (21). Despite the unknown factor(s), the clinical implications of this finding are even greater in patients, which are vastly more heterogeneous in their genetic background and tumor immunogenicity.

Clinical as well as experimental data suggest that the effects of local radiation may extend to tumors outside the treatment field. This abscopal effect was recently highlighted by a case report suggesting the possible role of adaptive immunity (22). These data are consistent with

the idea that local RT can induce immune responses to control local tumor cells but might also reduce the outgrowth of distant metastasis. However, more studies are needed to optimize the conditions for combination strategies utilizing RT and immunotherapy.

Recent studies point to an interesting role for T cells and IFN in achieving equilibrium in carcinogen-induced murine tumor models (9, 23–24). The underlying conclusions from these studies is that emerging tumors are immunologically selected, leaving behind clones that either lack expression of suitable antigens for T cell-mediated recognition (antigen-loss variants), or have evolved other mechanisms to resist immune attack (acquired resistance). Although immunological selection pressure could drive the selection of poorly antigenic clones (25–26), tumor outgrowth need not be accompanied by loss of antigenicity since tumors expressing tumor-specific or tumor-associated antigens have been documented in patients and spontaneous T cell responses against these antigens can be detected. Thus, established tumors can escape immune-mediated killing through mechanisms other than loss of antigen expression. In particular, many mechanisms of immune suppression are enlisted by the tumor to prevent adequate recognition including recruitment of suppressor cell subsets and upregulation or overexpression of T cell negative regulators such as PD-L1. Disruption of these acquired resistance mechanisms can uncover potent host immunity that can inhibit tumor progression or lead to complete regression, likely depending on various factors that affect the overall strength of the underlying host T cell response. It is clear that local radiation can, at least transiently, tip the balance of suppression back toward host immunity to generate a temporary state of equilibrium, the duration of which is affected by the state of host tolerance to expressed tumor antigens. Thus, tumors might actually proceed through several periods of equilibrium and escape both during the outgrowth of nascent tumors and again during treatment of the established tumor with cytotoxic therapies such as radiation. Our results suggest that radiation induced equilibrium is likely to be mediated by similar host mechanisms to equilibrium of nascent tumors, with host T cells and IFN being essential. Without further intervention, however, most irradiated tumors eventually escape due to, as yet, poorly defined mechanisms. We demonstrate that expression of PD-L1 in the irradiated tumor microenvironment is a critical barrier to host immunity, and therapeutic blockade with anti-PD-L1 antibody could disrupt equilibrium resulting in complete tumor regression in a high percentage of mice.

Emerging preclinical data are revealing how the host immune system sculpts the development of cancer (25–26). Preclinical data show that adoptively transferring tumor antigen-specific $CD4^+$ T cells can arrest multistage carcinogenesis in the dormant state through TNF and IFNγ signaling (27). However, there is very limited data addressing the potential role that anti-tumor immunity plays in partial response/stable disease that can be induced and maintained by radiotherapy. Even fewer studies utilize tumor equilibrium as a therapeutic window wherein host anti-tumor immunity is most amenable to therapeutic interventions.

T-cell exhaustion within the tumor microenvironment may be partially responsible for the stalemate that produces a period of radiographic stability following RT. New reports reveal that the inhibitory receptors PD-1 and Tim-3 are positively correlated with exhaustion of tumor-specific $CD8^+$ T cells in human and murine tumors (28–30). Furthermore, two recent clinical trials concluded that blockade of the PD-1 pathway can restore immune responses leading to tumor control in some advanced tumors that failed conventional therapies (31–32). Interestingly, anti-PD-L1 treatment fails to exhibit tumor growth inhibition if PD-L1 is not expressed within the local tumor tissue, and 36% patients with detectable expression of PD-L1 in tumor tissue respond to the treatment. We report that treatment of tumors with RT can induce the expression of PD-L1, and tumor infiltrating T cells often express PD-1 after RT. Based on the known inhibitory function of PD-1 on $CD8^+$ T cells, we demonstrate here

that PD-L1 blockade can break the equilibrium stalemate and tip the balance towards tumor regression. Direct activation of T cells within the tumor microenvironment could potentially be another strategy to clear RT-induced equilibrium tumors (18, 33).

Our results identify an active interplay between tumor cells and immune cells that occurs in RITE and suggest anti-PD-L1 antibody might have some utility in the treatment of radioresistant tumors. Furthermore our results demonstrate that the efficacy of RT can be potentiated by proper immunotherapy.

Supplementary Material

Refer to Web version on PubMed Central for supplementary material.

Acknowledgments

The authors acknowledge Drs. S.J. Kron and N.N. Khodarev for helpful scientific discussion

Funding: This research was in part supported by US National Institutes of Health grants CA141975 and CA97296 to Y.X.F, CA111423 to R.R.W., a grant from the Ludwig Foundation to R.R.W., and a generous gift from The Foglia Foundation (Y-X.F., and R.R.W.).

REFERENCES AND NOTES

1. Demicheli R, Biganzoli E, Boracchi P, Greco M, Retsky MW. Recurrence dynamics does not depend on the recurrence site. Breast Cancer Res. 2008; 10:R83. [PubMed: 18844974]
2. Klein CA. Framework models of tumor dormancy from patient-derived observations. Curr Opin Genet Dev. 2011; 21:42–49. [PubMed: 21145726]
3. Darby S, McGale P, Correa C, Taylor C, Arriagada R, Clarke M, Cutter D, Davies C, Ewertz M, Godwin J, Gray R, Pierce L, Whelan T, Wang Y, Peto R. Effect of radiotherapy after breast-conserving surgery on 10-year recurrence and 15-year breast cancer death: meta-analysis of individual patient data for 10,801 women in 17 randomised trials. Lancet. 2011; 378:1707–1716. [PubMed: 22019144]
4. Pilepich MV, Winter K, Lawton CA, Krisch RE, Wolkov HB, Movsas B, Hug EB, Asbell SO, Grignon D. Androgen suppression adjuvant to definitive radiotherapy in prostate carcinoma--long-term results of phase III RTOG 85–31. Int J Radiat Oncol Biol Phys. 2005; 61:1285–1290. [PubMed: 15817329]
5. Char DH, Kroll S, Phillips TL, Quivey JM. Late radiation failures after iodine 125 brachytherapy for uveal melanoma compared with charged-particle (proton or helium ion) therapy. Ophthalmology. 2002; 109:1850–1854. [PubMed: 12359605]
6. Chao KS, Ozyigit G, Tran BN, Cengiz M, Dempsey JF, Low DA. Patterns of failure in patients receiving definitive and postoperative IMRT for head-and-neck cancer. Int J Radiat Oncol Biol Phys. 2003; 55:312–321. [PubMed: 12527043]
7. Aguirre-Ghiso JA. Models, mechanisms and clinical evidence for cancer dormancy. Nat Rev Cancer. 2007; 7:834–846. [PubMed: 17957189]
8. Goss PE, Chambers AF. Does tumour dormancy offer a therapeutic target? Nat Rev Cancer. 2010; 10:871–877. [PubMed: 21048784]
9. Koebel CM, Vermi W, Swann JB, Zerafa N, Rodig SJ, Old LJ, Smyth MJ, Schreiber RD. Adaptive immunity maintains occult cancer in an equilibrium state. Nature. 2007; 450:903–907. [PubMed: 18026089]
10. Salama JK, Chmura SJ, Mehta N, Yenice KM, Stadler WM, Vokes EE, Haraf DJ, Hellman S, Weichselbaum RR. An initial report of a radiation dose-escalation trial in patients with one to five sites of metastatic disease. Clin Cancer Res. 2008; 14:5255–5259. [PubMed: 18698045]
11. Salama JK, Hasselle MD, Chmura SJ, Malik R, Mehta N, Yenice KM, Villaflor VM, Stadler WM, Hoffman PC, Cohen EE, Connell PP, Haraf DJ, Vokes EE, Hellman S, Weichselbaum RR. Stereotactic body radiotherapy for multisite extracranial oligometastases: final report of a dose

escalation trial in patients with 1 to 5 sites of metastatic disease. Cancer. 2012; 118:2962–2970. [PubMed: 22020702]

12. Lee Y, Auh SL, Wang Y, Burnette B, Wang Y, Meng Y, Beckett M, Sharma R, Chin R, Tu T, Weichselbaum RR, Fu YX. Therapeutic effects of ablative radiation on local tumor require CD8+ T cells: changing strategies for cancer treatment. Blood. 2009; 114:589–595. [PubMed: 19349616]
13. Park S, Jiang Z, Mortenson ED, Deng L, Radkevich-Brown O, Yang X, Sattar H, Wang Y, Brown NK, Greene M, Liu Y, Tang J, Wang S, Fu YX. The therapeutic effect of anti-HER2/neu antibody depends on both innate and adaptive immunity. Cancer Cell. 2010; 18:160–170. [PubMed: 20708157]
14. Burnette BC, Liang H, Lee Y, Chlewicki L, Khodarev NN, Weichselbaum RR, Fu YX, Auh SL. The efficacy of radiotherapy relies upon induction of type i interferon-dependent innate and adaptive immunity. Cancer Research. 2011; 71:2488–2496. [PubMed: 21300764]
15. Lugade AA, Sorensen EW, Gerber SA, Moran JP, Frelinger JG, Lord EM. Radiation-induced IFN-gamma production within the tumor microenvironment influences antitumor immunity. Journal of immunology (Baltimore, Md : 1950). 2008; 180:3132–3139.
16. Wherry EJ. T cell exhaustion. Nat Immunol. 2011; 12:492–499. [PubMed: 21739672]
17. Curiel TJ, Wei S, Dong H, Alvarez X, Cheng P, Mottram P, Krzysiek R, Knutson KL, Daniel B, Zimmermann MC, David O, Burow M, Gordon A, Dhurandhar N, Myers L, Berggren R, Hemminki A, Alvarez RD, Emilie D, Curiel DT, Chen L, Zou W. Blockade of B7-H1 improves myeloid dendritic cell-mediated antitumor immunity. Nat Med. 2003; 9:562–567. [PubMed: 12704383]
18. Zou W, Chen L. Inhibitory B7-family molecules in the tumour microenvironment. Nat Rev Immunol. 2008; 8:467–477. [PubMed: 18500231]
19. Wolstenholme JT, Warner JA, Capparuccini MI, Archer KJ, Shelton KL, Miles MF. Genomic analysis of individual differences in ethanol drinking: evidence for non-genetic factors in C57BL/6 mice. PLoS One. 2011; 6:e21100. [PubMed: 21698166]
20. Koolhaas JM, de Boer SF, Coppens CM, Buwalda B. Neuroendocrinology of coping styles: towards understanding the biology of individual variation. Front Neuroendocrinol. 2010; 31:307–321. [PubMed: 20382177]
21. Martin ME, Dieter JA, Luo Z, Baumgarth N, Solnick JV. Predicting the outcome of infectious diseases: variability among inbred mice as a new and powerful tool for biomarker discovery. MBio. 2012; 3:e00199–00112. [PubMed: 23073762]
22. Postow MA, Callahan MK, Barker CA, Yamada Y, Yuan J, Kitano S, Mu Z, Rasalan T, Adamow M, Ritter E, Sedrak C, Jungbluth AA, Chua R, Yang AS, Roman RA, Rosner S, Benson B, Allison JP, Lesokhin AM, Gnjatic S, Wolchok JD. Immunologic correlates of the abscopal effect in a patient with melanoma. The New England journal of medicine. 2012; 366:925–931. [PubMed: 22397654]
23. Dunn GP, Koebel CM, Schreiber RD. Interferons, immunity and cancer immunoediting. Nat Rev Immunol. 2006; 6:836–848. [PubMed: 17063185]
24. Schreiber RD, Old LJ, Smyth MJ. Cancer immunoediting: integrating immunity's roles in cancer suppression and promotion. Science. 2011; 331:1565–1570. [PubMed: 21436444]
25. Matsushita H, Vesely MD, Koboldt DC, Rickert CG, Uppaluri R, Magrini VJ, Arthur CD, White JM, Chen YS, Shea LK, Hundal J, Wendl MC, Demeter R, Wylie T, Allison JP, Smyth MJ, Old LJ, Mardis ER, Schreiber RD. Cancer exome analysis reveals a T-cell-dependent mechanism of cancer immunoediting. Nature. 2012; 482:400–404. [PubMed: 22318521]
26. DuPage M, Mazumdar C, Schmidt LM, Cheung AF, Jacks T. Expression of tumour-specific antigens underlies cancer immunoediting. Nature. 2012; 482:405–409. [PubMed: 22318517]
27. Muller-Hermelink N, Braumuller H, Pichler B, Wieder T, Mailhammer R, Schaak K, Ghoreschi K, Yazdi A, Haubner R, Sander CA, Mocikat R, Schwaiger M, Forster I, Huss R, Weber WA, Kneilling M, Rocken M. TNFR1 signaling and IFN-gamma signaling determine whether T cells induce tumor dormancy or promote multistage carcinogenesis. Cancer Cell. 2008; 13:507–518. [PubMed: 18538734]
28. Zhou Q, Munger ME, Veenstra RG, Weigel BJ, Hirashima M, Munn DH, Murphy WJ, Azuma M, Anderson AC, Kuchroo VK, Blazar BR. Coexpression of Tim-3 and PD-1 identifies a CD8+ T-

cell exhaustion phenotype in mice with disseminated acute myelogenous leukemia. Blood. 2011; 117:4501–4510. [PubMed: 21385853]

29. Sakuishi K, Apetoh L, Sullivan JM, Blazar BR, Kuchroo VK, Anderson AC. Targeting Tim-3 and PD-1 pathways to reverse T cell exhaustion and restore anti-tumor immunity. J Exp Med. 2010; 207:2187–2194. [PubMed: 20819927]
30. Fourcade J, Sun Z, Benallaoua M, Guillaume P, Luescher IF, Sander C, Kirkwood JM, Kuchroo V, Zarour HM. Upregulation of Tim-3 and PD-1 expression is associated with tumor antigen-specific CD8+ T cell dysfunction in melanoma patients. J Exp Med. 2010; 207:2175–2186. [PubMed: 20819923]
31. Brahmer JR, Tykodi SS, Chow LQ, Hwu WJ, Topalian SL, Hwu P, Drake CG, Camacho LH, Kauh J, Odunsi K, Pitot HC, Hamid O, Bhatia S, Martins R, Eaton K, Chen S, Salay TM, Alaparthy S, Grosso JF, Korman AJ, Parker SM, Agrawal S, Goldberg SM, Pardoll DM, Gupta A, Wigginton JM. Safety and activity of anti-PD-L1 antibody in patients with advanced cancer. N Engl J Med. 2012; 366:2455–2465. [PubMed: 22658128]
32. Topalian SL, Hodi FS, Brahmer JR, Gettinger SN, Smith DC, McDermott DF, Powderly JD, Carvajal RD, Sosman JA, Atkins MB, Leming PD, Spigel DR, Antonia SJ, Horn L, Drake CG, Pardoll DM, Chen L, Sharfman WH, Anders RA, Taube JM, McMiller TL, Xu H, Korman AJ, Jure-Kunkel M, Agrawal S, McDonald D, Kollia GD, Gupta A, Wigginton JM, Sznol M. Safety, activity, and immune correlates of anti-PD-1 antibody in cancer. N Engl J Med. 2012; 366:2443–2454. [PubMed: 22658127]
33. Croft M. The role of TNF superfamily members in T-cell function and diseases. Nature reviews Immunology. 2009; 9:271–285.

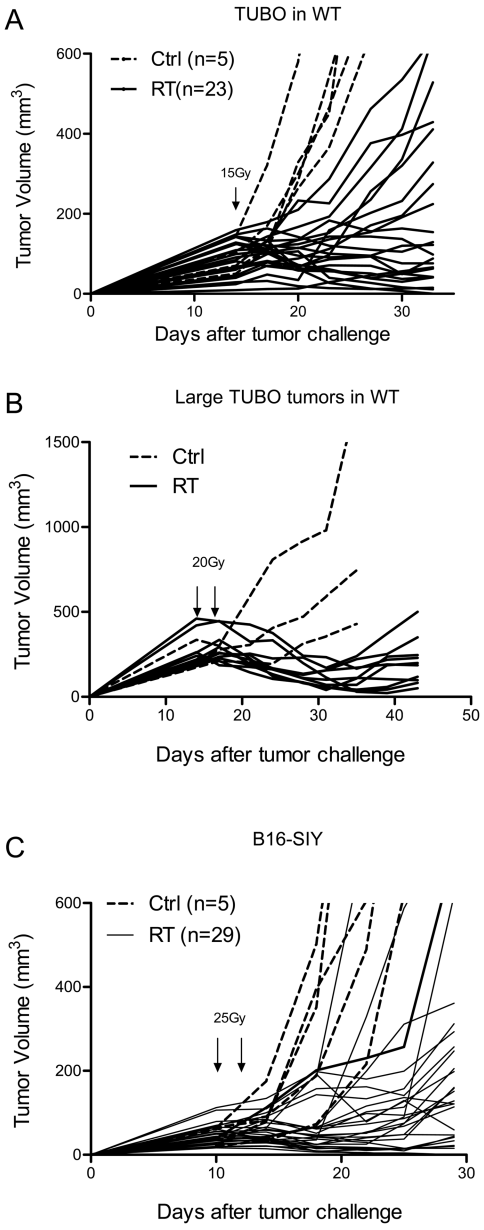

Figure 1.

Ablative RT controls local tumor and induce stable/equilibrium diseases. (**A**) Balb/c wild type mice were s.c. inoculated with 5×10^5 TUBO. Tumors were irradiated with 15Gy 14 days later. **(B)** Larger TUBO tumors (200–400mm^3) could be induced into equilibrium by higher dose of radiation. **(C)** B16-SIY tumors were allowed to grow for 10 days and then treated by two doses of 25Gy. Dotted lines: 0Gy control; solid lines: individual tumors received radiation. One of eight **(A)**, two **(B, C)** representative experiments, respectively, is shown.

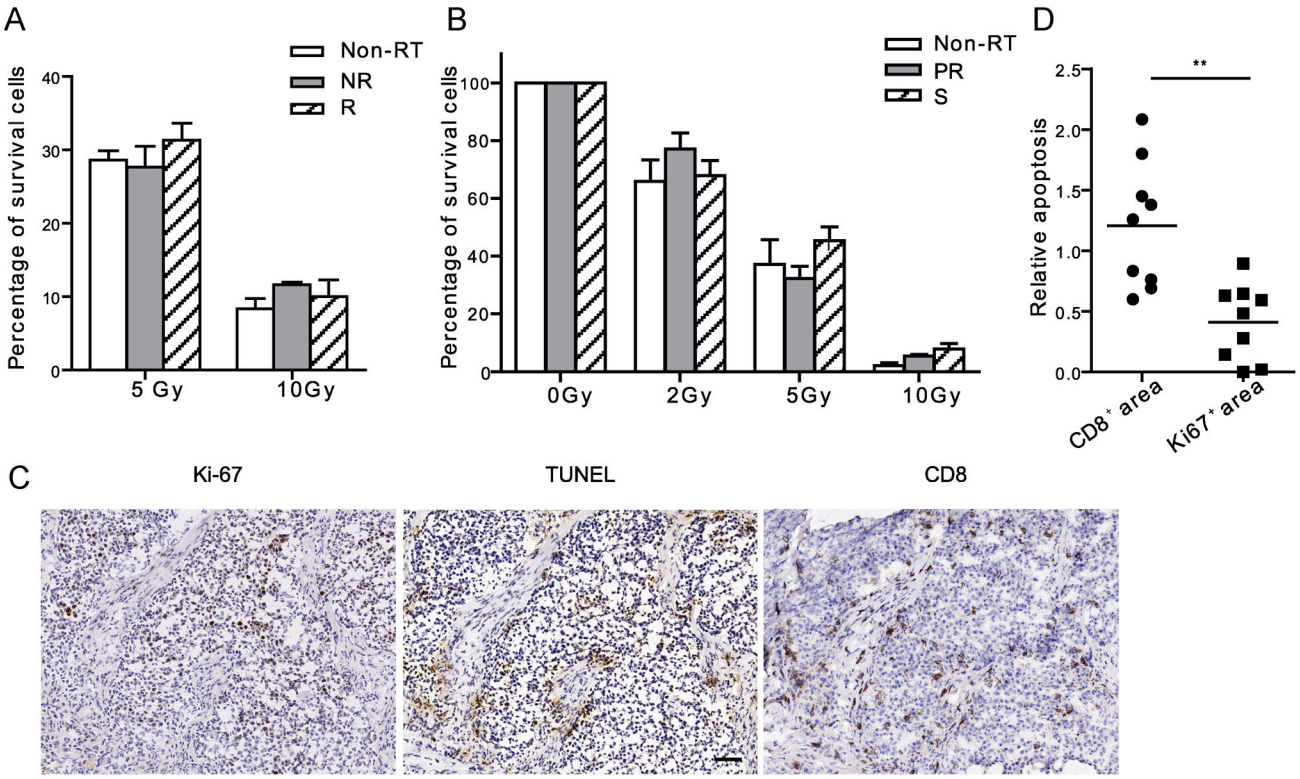

Figure 2.

Host immune responses, not the radiosensitivity of cancer cells, correlate with efficacy of RT. **(A)** Tumor cells had the equal level of the sensitivity to radiation despite their differential early response to RT in vivo. Eight days after RT, non-RT control, non-responsive (NR) and responsive (R) tumors were removed and digested into cell suspension. The cells received 0Gy, 5Gy or 10Gy, and cultured for 7 days. Clonogenic assay was performed. **(B)** 21 days post RT, tumors were excised from partial response (PR), Stable (S) and Non-RT hosts and digested into cell suspension. The cells received 0Gy, 2Gy, 5Gy or 10Gy. Survival clonogenic assay was performed. The data was graphed as percentage compared to number of colonies in 0Gy control of each type of tumor. **(C)** IHC assay of the sequential slides of stable tumors stained with Ki-67, TUNEL and CD8 antibodies. Scale bar, 50μm. (**D**) Quantification of relative intensity of TUNEL staining in $CD8^+$ and $Ki67^+$ areas, 3–4 high power fields were counted per mouse. n=3. ** P=0.001. **One of** two **(A, B)** representative experiments is shown.

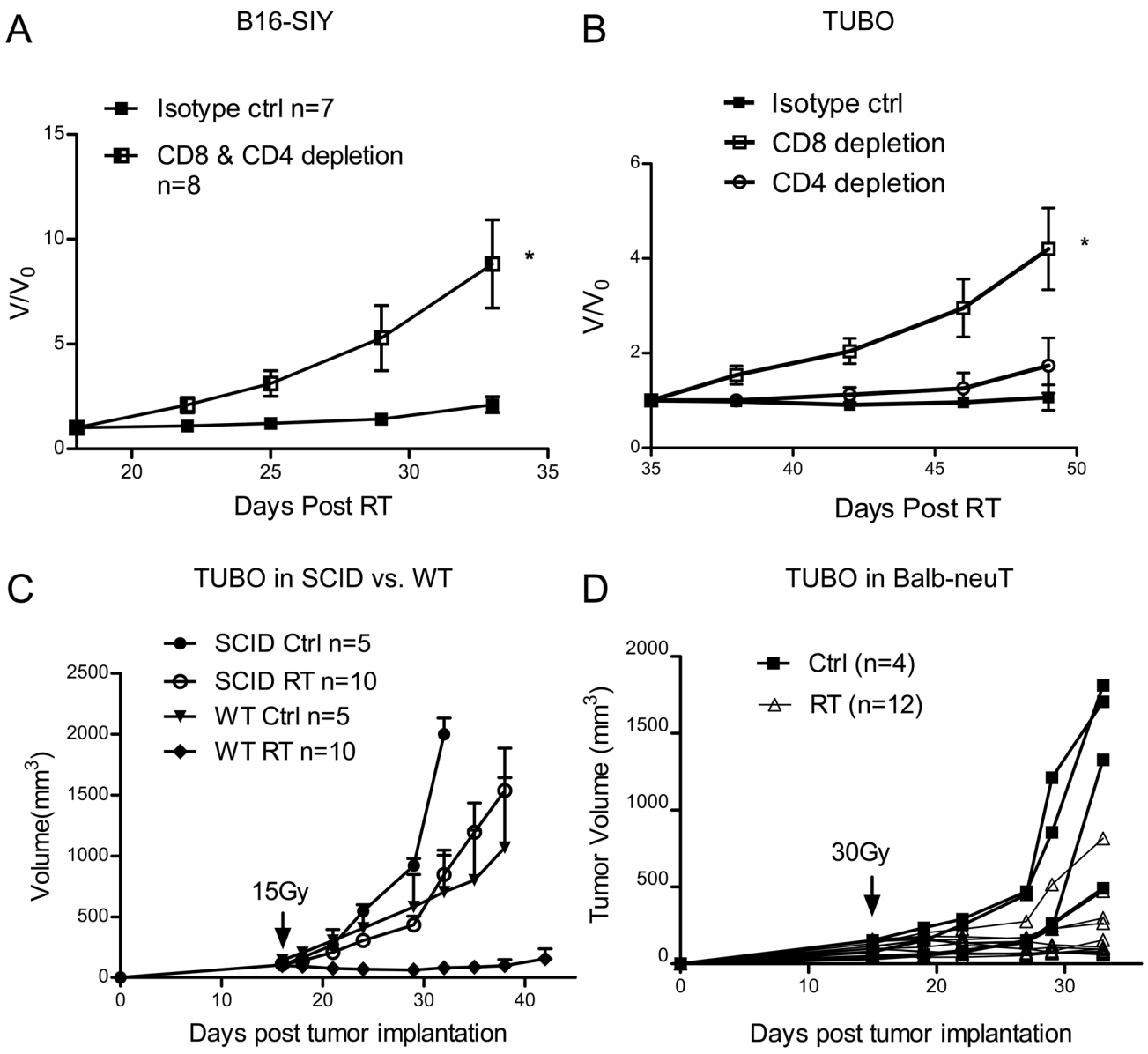

Figure 3.

Antigen specific T cell responses are required for maintaining stable diseases. **(A)** Eighteen days after RT, $CD8^+$ and $CD4^+$ T cells were depleted in stable B16-SIY tumor. $^*p=0.016$, n=8. V_0 represents the tumor volume at the day of starting antibody treatment and V represents the tumor volume after antibody treatment. **(B)** Thirty five days after RT, mice with stable TUBO tumor were selected and depleted of CD8 or CD4 cells. *P=0.015, n=8. **(C)** Unlike in WT host, TUBO tumors in SCID mice could not reach equilibrium. Mice were treated as Fig. 1A. n=10. **(D)** TUBO tumors in BALB-neuT can be induced into equilibrium by RT. Tumors were irradiated with 30Gy 15 days later. Tumors in individual mouse were shown. One of two **(A, C, D)** or three **(B)** representative experiments is shown, respectively.

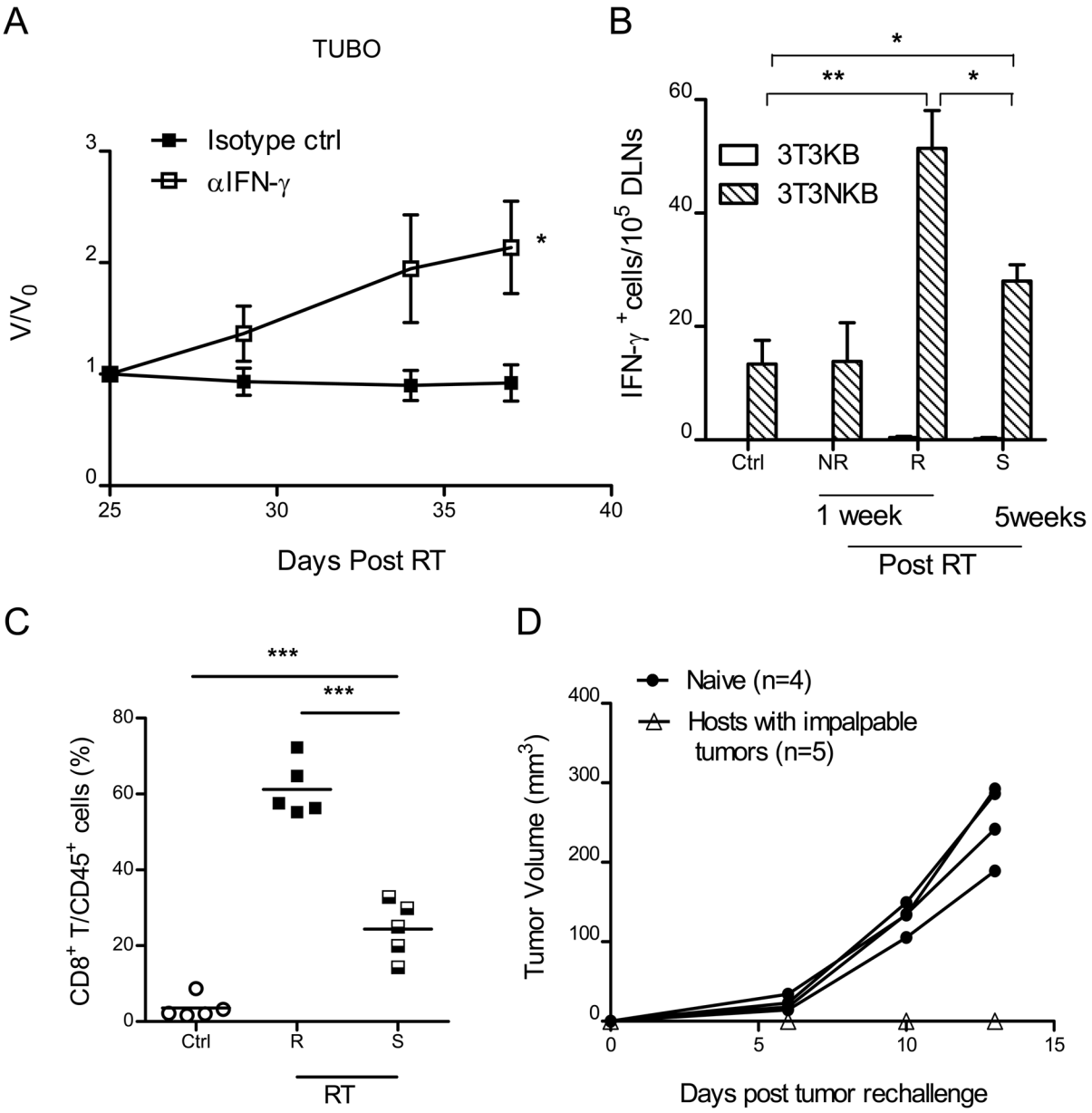

Figure 4.

Antigen specific T cell responses are required for RT response as well as maintaining stable diseases. **(A)** Twenty five days after RT, mice bearing stable TUBO tumor were injected with IFNγ neutralizing antibody. *P=0.026, n=7. **(B)** Increased T cell response to neu antigen in DLNs in animals with responder tumors and stable tumors. DLNs were collected from control (non-RT group), non-responsive (NR), responsive group (R) 1 week after RT and stable group (S) 5 weeks after RT. IFNγ ELISPOT assays were performed. 3T3NKB cells were used for antigen presentation, 3T3KB as non-specific antigen control. *P<0.05, **P= 0.001, n=3/group. **(C)** $CD8^+$ T cell frequency in both responder and stable tumors from **(B)** are elevated. ***P≤0.0005. (**D**) Systemic memory T cell response protects hosts from tumor re-challenge. Mice were re-challenged with 2×10^6 Tubo cells on the opposite flank 30 days after tumors were impalpable. One of three representative experiments is shown.

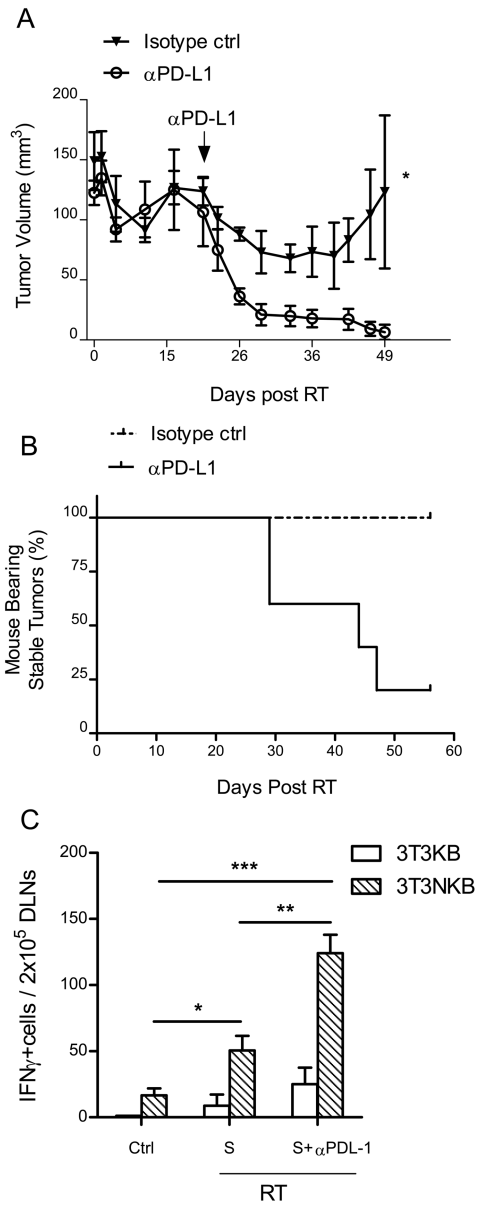

Figure 5.

Blockade of PD-L1 breaks the equilibrium to favor tumor regression. Tumors were implanted and irradiated as Fig. 1A. Antibodies were administered 21 days after RT. (A) Tumors regressed after anti-PD-L1 injections. (B) Mice in treated group became tumor free over time. *P=0.018, n=5/group; (**C**) Antigen specific functional T cells were highly activated in stable tumors after neutralization of PD-L1. DLN of 4 mice per group were excised 5 weeks post RT (S) or 1 week post PD-L1 blockade (S+αPD-L1) and subjected to ELISPOT assays. *P=0.047; **P=0.002; ***P=0.0003. One of three representative experiments is shown.